PCCP

RSC Publishing

COMMUNICATION

Environment-driven reactivity of H_2 on PdRu surface alloys†

Cite this: *Phys. Chem. Chem. Phys.*, 2013, **15**, 14936

Received 11th May 2013,
Accepted 12th July 2013

DOI: 10.1039/c3cp52001c

www.rsc.org/pccp

M. Ramos,[a] M. Minniti,[b] C. Díaz,[c] D. Farías,[b] R. Miranda,[bd] F. Martín,[cd] A. E. Martínez[a] and H. F. Busnengo*[a]

The dissociative adsorption of molecular hydrogen on Pd_xRu_{1-x}/Ru(0001) ($0 \leq x \leq 1$) has been investigated by means of He atom scattering, Density Functional Theory and quasi-classical trajectory calculations. Regardless of their surroundings, Pd atoms in the alloy are always less reactive than Ru ones. However, the reactivity of Ru atoms is enhanced by the presence of nearest neighbor Pd atoms. This environment-dependent reactivity of the Ru atoms in the alloy provides a sound explanation for the striking step-like dependence of the initial reactive sticking probability as a function of the Pd concentration observed in experiments. Moreover, we show that these environment-dependent effects on the reactivity of H_2 on single atoms allow one to get around the usual constraint imposed by the Brønsted–Evans–Polanyi relationship between the reaction barrier and chemisorption energy.

Bimetallic surface alloys offer great flexibility to design interfaces with specific properties, which explains the great deal of attention they have attracted during the last years.[1–12] Through the use of physical vapor deposition at different surface temperatures and/or selecting adequate annealing conditions, it is possible to control the amount of ad-atoms deposited on a host surface, as well as their location and surroundings.[7,8] This opens the door to unprecedented investigations on the reactivity of isolated atoms and/or small aggregates of a catalytic species,[10] which will help filling the gap between *real-world* surfaces and the ideal single-component ones usually considered in surface science studies.[13]

Pd_xRu_{1-x}/Ru(0001) ($0 \leq x \leq 1$) are surface alloys of particular interest (here $x = 0$ and $x = 1$ correspond to pure Ru(0001) and Pd_{ML}/Ru(0001) respectively). Thanks to the pseudomorphic growth of Pd on Ru(0001) in a wide range of temperatures, in the submonolayer regime it is possible to achieve precise control of the Pd coverage using He atom scattering (HAS)[14] (see Fig. S1 in the ESI†) and scanning tunneling microscopy (STM).[7] Flash annealing to $\sim$1100 K gives rise to a single-layer PdRu alloy characterized by phase separation into 2D Pd and Ru islands and well defined Pd/Ru relative contents.[7] Whereas for a wide range of intermediate Pd concentrations ($0.15 < x < 0.85$) Ru- and Pd-aggregates of various different sizes coexist, for Ru-rich (Pd-rich) alloys almost all the Pd (Ru) atoms are isolated, *i.e.* fully surrounded by Ru (Pd) atoms.

For Pd_xRu_{1-x}/Ru(0001) alloys with x increasing from 0 to 1 the D_2 desorption temperature, T_{des}, smoothly decreases from $\sim$400 K to $\sim$250 K, which corresponds to a decrease of the atomic hydrogen binding energy from $\sim$0.52 eV to $\sim$0.31 eV.[15] In contrast, the initial reactive sticking coefficient, s_0, of D_2 molecules at room temperature (RT) on Pd_xRu_{1-x}/Ru(0001) remains constant for a wide range of Pd concentrations (for $0 \leq x \lesssim 0.9$), and suddenly decreases when Pd covers almost completely the Ru(0001) substrate (see Fig. 1a). This step-like dependence was first observed by Hartmann and co-workers who determined s_0 by computing the derivative of the measured D-coverage *vs.* D_2-exposure curve in the limit of zero exposure for alloys with various Pd concentrations.[7] The HAS technique allows us to determine not only the amount of deposited Pd with a daily precision of *ca.* 1% but also relative values of s_0 that is proportional to the initial slope of the deposition curve.[16] Thus, using a HAS experimental set-up,[14] we have investigated the reactivity of H_2 on Pd_xRu_{1-x}/Ru(0001) by monitoring the specularly reflected He beam intensity while exposing the sample to a H_2 background pressure (see Fig. 1b). As we can see in Fig. 1b, essentially the same deposition curve is obtained for both $Pd_{0.95}Ru_{0.05}$/Ru(0001) and Ru(0001). In contrast, in the case of Pd_{ML}/Ru(0001) the slope of the deposition curve is smaller by a factor of $\sim$4, which is compatible with the step-like behavior of s_0 as a function of x reported in ref. 7.

[a] *Grupo de Fisicoquímica en Interfases y Nanoestructuras, Instituto de Física Rosario and Universidad Nacional de Rosario, 2000 Rosario, Argentina. E-mail: busnengo@ifir-conicet.gov.ar*
[b] *Departamento de Física de la Materia Condensada, and Instituto Nicolás Cabrera, Universidad Autónoma de Madrid, 28049 Madrid, Spain*
[c] *Departamento de Química, Universidad Autónoma de Madrid, 28049 Madrid, Spain*
[d] *Instituto Madrileño de Estudios Avanzados en Nanociencia (IMDEA-Nanociencia), 28049 Madrid, Spain*

† Electronic supplementary information (ESI) available. See DOI: 10.1039/c3cp52001c

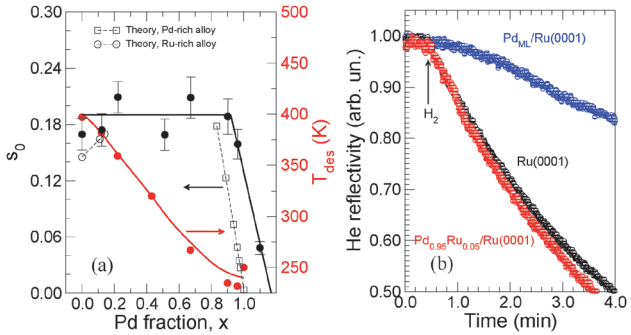

Fig. 1 (a) Sticking probability, s_0 (black), and desorption temperature, T_{des} (red), as a function of the Pd fraction for molecular hydrogen interacting with Pd_xRu_{1-x}/Ru(0001). Full symbols: experimental data taken from ref. 7, open symbols: theoretical results for H_2 (present work). The arrows indicate the *y*-axis corresponding to s_0 (left) and T_{des} (right), and the lines are guides for the eye. (b) Intensity of the He specular peak as a function of time during exposition of Ru(0001), $Pd_{0.95}Ru_{0.05}$/Ru(0001), and Pd_{ML}/Ru(0001) to H_2 background pressure (present work). The surface alloy $Pd_{0.95}Ru_{0.05}$/Ru(0001) was annealed to 1150 K before recording the data at 120 K. The arrow indicates the beginning of the H_2 dosing.

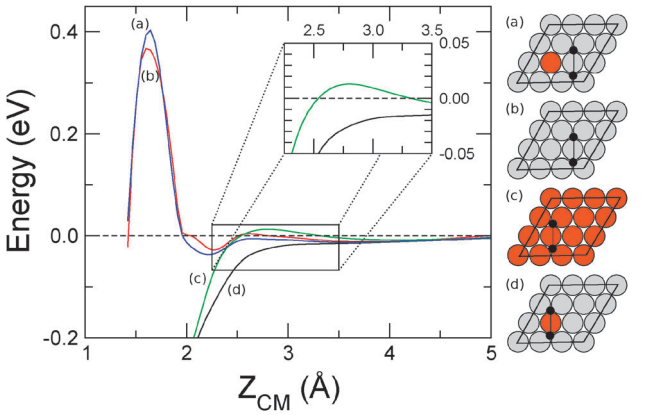

Fig. 2 Potential energy along four 2D(r,Z_{CM}) H_2 DPs as a function of Z_{CM}: (a) and (d) $Pd_{0.89}Ru_{0.11}$/Ru(0001), (b) Pd_{ML}/Ru(0001), and (c) Ru(0001) surfaces. The molecular configurations for which each DP has been computed are depicted in the panels on the right, where orange (grey) circles represent Ru (Pd) atoms.

Previous Density Functional Theory (DFT) and quasi-classical trajectory (QCT) calculations have anticipated a very small reactivity of Pd_{ML}/Ru(0001) (x = 1) under exposure to low energy molecular hydrogen, which is due to an activation energy barrier of $\sim$0.2 eV,[5] *i.e.* one order of magnitude larger than on Ru(0001) (x = 0).[17–19] Due to both strain and electronic ligand effects, in Pd_{ML}/Ru(0001) Pd atoms lose their natural high capacity to spontaneously dissociate H_2.[5] Therefore, the progressive replacement of Ru atoms by the *less reactive* Pd ones is expected to entail a progressive decrease of s_0. Moreover, if we take into account the general Brønsted–Evans–Polanyi (BEP) linear relationship between the activation energy for dissociation and the dissociative chemisorption energy,[20,21] and the measured smooth decrease of the atomic hydrogen binding energy with increasing x, a similar smooth decrease of s_0 is expected instead of the step-like behavior observed in experiments.

In this paper we show that this striking dependence can be explained in terms of a subtle environment-dependent reactivity of Ru atoms in the Pd_xRu_{1-x}/Ru(0001) alloys. Whereas the Pd atoms in these alloys are themselves unreactive, they turn their nearest neighbor (NN) Ru atoms more reactive than in pure Ru(0001). Thus, for instance, a relatively small fraction of isolated Ru atoms in a Pd-rich alloy (*e.g.* $x \sim 0.95$) provokes a global reactivity much higher than that of the full Pd overlayer (x = 1) and similar to that of pure Ru(0001) (x = 0). On the other hand, for low and intermediate Pd concentrations, an increase in the fraction of unreactive Pd atoms is compensated by the increased reactivity they induce in their NN Ru atoms.

We have performed DFT calculations using the Vienna *ab initio* Simulation Package (VASP)[22–24] which makes use of a plane-wave basis set to represent the Kohn–Sham orbitals. We have used the projector augmented-wave method[25] to describe the interaction of the valence electrons with the atomic cores, and the Perdew–Burke–Ernzerhof (PBE)[26] exchange–correlation functional. The energy cutoff employed was 400 eV and electronic smearing was introduced following the Methfessel and Paxton approach[27] with N = 1 and σ = 0.2. This setup gives lattice parameters of Ru bulk (a = 2.71 Å and c = 4.28 Å) in excellent agreement with the experimental ones (a^{exp} = 2.70 Å and c^{exp} = 4.28 Å).[28] The surface alloy Pd_xRu_{1-x}/Ru(0001) ($0 \leq x \leq 1$) was represented by a five-layer slab separated from its periodic images by a 16 Å width vacuum region. The two bottom layers of the slab were kept fixed at the theoretical bulk distance between consecutive (0001) planes of Ru, $d_{0001} = c/2$, whereas the positions of the remaining atoms were fully optimized (in the absence of hydrogen). All the DFT calculations were carried out for a 3 × 3 unit cell using a 7 × 7 × 1 Γ-centered k-points grid.

In Fig. 2 we show four dissociation pathways (DPs) for: H_2/$Pd_{0.89}Ru_{0.11}$/Ru(0001) (a) and (d), H_2/Pd_{ML}/Ru(0001) (b), and H_2/Ru(0001) (c). These pathways have been computed within 2D(r,Z_{CM}) cuts of the potential energy surfaces (PES), with r and Z_{CM} being the H–H distance and the height of the molecular center of the mass above the surface respectively. In all the cases considered in Fig. 2 the molecule is parallel to the surface, its center of mass is placed on top of a Pd atom (panels a and b) and on top of a Ru atom (panels c and d), and the H–H bond points to nearest *hollow-fcc* and *hollow-hcp* sites. In what follows, such molecular configurations will be referred to as fcc-topPd-hcp and fcc-topRu-hcp respectively.

In agreement with DFT-PW91[29] results reported previously for H_2/Ru(0001)[17] and H_2/Pd_{ML}/Ru(0001),[5] the present DFT-PBE calculations predict that H_2 dissociation on both surfaces is an activated process. In the former case, the minimum activation energy barrier is $\sim$0.015 eV and is located early in the entrance channel $Z_{CM} \sim$ 3 Å (see curve (c) in Fig. 2) whereas in the latter case the minimum activation energy barrier (found for fcc-bridge-hcp configurations) is $\sim$0.2 eV.[5] In contrast, isolated Ru atoms in the Pd-rich surface alloy $Pd_{0.89}Ru_{0.11}$/Ru(0001) offer a non-activated dissociation pathway for impinging H_2 molecules, see Fig. 2(d). For the Pd_xRu_{1-x}/Ru(0001) alloys with different Pd concentrations investigated (x = 0, 0.11, 0.22, 0.78, 0.89, and 1), we have found that

the most stable sites for atomic hydrogen chemisorption (after molecular dissociation) are always (threefold) hollow-fcc. In addition, hydrogen atoms always prefer adsorption in the local environment with the largest number of Ru atoms around them. This trend is likely to be connected with the small but systematic up-shift of the center of the d-band projected on topmost-layer Ru atoms when the number of NN Pd atoms increases (see the ESI† for further details).

Interestingly, the DPs for the fcc-topPd-hcp configuration on both $Pd_{0.89}Ru_{0.11}$/Ru(0001) and Pd_{ML}/Ru(0001) are very similar to each other, and despite the relatively large activation energy barrier ($\sim$0.40 eV), low energy molecules can approach the surface (down to $Z_{CM} \sim 2$ Å) without experiencing any repulsion (curves (a) and (b) in Fig. 2). The DPs obtained for the fcc-bridgePdPd-hcp configuration (*i.e.* with the molecular center of mass on a bridge site between NN Pd atoms and the H–H bond pointing to the closest fcc and hcp sites, not shown) on $Pd_{0.89}Ru_{0.11}$/Ru(0001) and Pd_{ML}/Ru(0001) are also similar to each other. This is a consequence of the strongly localized character of the *perturbation* introduced by isolated Ru atoms into the Pd monolayer. This perturbation can be properly accounted for by the attractive pairwise Ru–H potential, V_{Ru-H}, shown in Fig. 3(a). Accordingly, for Pd-rich surface alloys ($x \gtrsim 0.85$) the 6D-PES of H_2/Pd_xRu_{1-x}/Ru(0001), V_{6D}^x, can be approximated as:

$$V_{6D}^x = V_{6D}^{x=1} + \sum_i V_{Ru-H}(R_{i,1}) + V_{Ru-H}(R_{i,2}), \qquad (1)$$

where $V_{6D}^{x=1}$ is the 6D-PES of H_2/Pd_{ML}/Ru(0001) described in ref. 30, $R_{i,j}$ is the distance between the jth atom of the molecule (j = 1,2) and the ith Ru atom, and the sum is over all the Ru atoms in the outermost surface layer. The accuracy of this model is illustrated in Fig. 3(b–d) where we compare the values

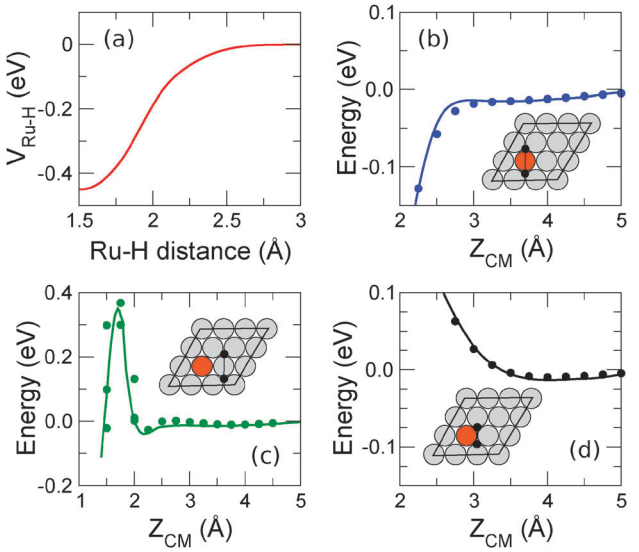

Fig. 3 (a) Ru–H pairwise potential, V_{Ru-H} (see text). (b–d) Comparison of the results obtained for the potential energy along various 2D(r,Z_{CM}) H_2 DPs. Solid lines: model potential V_{6D}^x for x = 0.89; full circles: DFT data. The molecular configurations (parallel to the surface) are illustrated in the insets, where orange (grey) circles represent Ru (Pd) atoms.

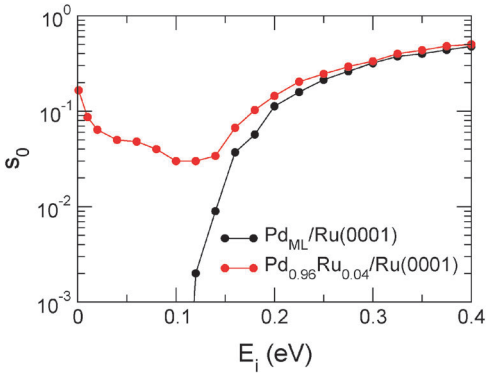

Fig. 4 Results for $H_2(\nu = 0, J = 0)$ initial sticking probability, s_0, on Pd_xRu_{1-x}/Ru(0001) for x = 0.96 and x = 1, as a function of the molecular impact energy, E_i, at normal incidence.

of $V_{6D}^{x=0.89}$ obtained using eqn (1) with DFT data along the DPs for the configurations depicted in the insets. In particular, eqn (1) properly accounts for the existence of non-activated DPs on top of Ru atoms for $Pd_{0.89}Ru_{0.11}$/Ru(0001) as well as the short-range influence of these Ru atoms.

At high Pd concentrations ($x \gtrsim 0.85$), Ru atoms in the PdRu surface alloy are far away from each other.[7] This allowed us to use V_{6D}^x (eqn (1)) in QCT calculations[31] of s_0 for H_2 and D_2 on Pd_xRu_{1-x}/Ru(0001) with $0.83 \leq x \leq 1$. We have computed s_0 as a function of the molecular impact energy, E_i, for normal incidence, and initial rovibrational states ν = 0, J = 0,1,2,3. We have considered Pd-rich surface alloy structures with only one outermost layer Ru atom per 2 × 3 and $n \times n$ unit cells (with n = 3,4,5,6,7) using periodic boundary conditions. We have assumed that surface atoms remain *frozen* in their equilibrium positions during the dynamics (*i.e.* static surface approximation), and for each (E_i, J) initial condition we have integrated 5000 trajectories. The results obtained for $H_2(\nu = 0, J = 0)/Pd_{0.96}Ru_{0.04}$/Ru(0001) are compared with those for $H_2(\nu = 0, J = 0)/Pd_{ML}$/Ru(0001) ($x$ = 1) in Fig. 4.[32] For $E_i >$ 0.15 eV, the s_0 values obtained for the two systems are very similar to each other: $s_0^{x=0.96} \sim s_0^{x=1} + 0.03$. The monotonously increasing dependence of $s_0(E_i)$ is a consequence of direct dissociation on both surfaces, and the 0.03 difference found is consistent with the 4% of active Ru atoms in the outermost layer of the alloy. Below $E_i \sim 0.12$ eV, $s_0^{x=1}$ is equal to zero[33] in stark contrast with the case of $H_2/Pd_{0.96}Ru_{0.04}$/Ru(0001). For $E_i < 0.1$ eV, $s_0^{x=0.96}$ increases when E_i decreases and reaches $\sim$0.2 for $E_i \sim 0$. This initial negative slope of $s_0^{x=0.96}(E_i)$ is a typical fingerprint of an indirect dissociation mechanism usually called dynamic trapping.[34] Trapped molecules can explore the surface for a while which increases the probability of finding the Ru active sites. Thus, for low energy molecules a small fraction of Ru atoms drastically enhances the reactivity of the Pd_xRu_{1-x}/Ru(0001) surface alloys with respect to the full Pd monolayer.

For a direct comparison with experiments we have also computed the reactive initial sticking probability averaged over E_i and various possible J initial states according to a gas of

hydrogen molecules at RT. These RT-averaged results for H_2 are shown in Fig. 1a (open squares).[35] In spite of a small shift down in x and a slightly larger (negative) slope of the theoretical results, the agreement with experiments is excellent. The sharp experimental decrease of s_0 observed for $x \sim 1$ is nicely reproduced by our QCT calculations.

We now turn our attention to the region of low Pd concentrations, where s_0 is nearly independent of x. To understand this behavior, we have carried out DFT calculations for $H_2/Pd_{0.11}Ru_{0.89}/Ru(0001)$ and $H_2/Pd_{0.22}Ru_{0.78}/Ru(0001)$ considering isolated Pd atoms and Pd dimers respectively. Similarly to the case of $Pd_{ML}/Ru(0001)$,[5] we have found that Pd atoms surrounded by Ru atoms are quite inert: *e.g.* the activation energy barrier for H_2 dissociation on $Pd_{0.11}Ru_{0.89}/Ru(0001)$ for the fcc-topPd-hcp configuration is $\sim$0.23 eV (see Fig. S5 in the ESI†). Interestingly, Fig. 5 also shows that the early $\sim$0.015 eV activation energy barrier found for the fcc-topRu-hcp configuration on pure Ru(0001) (curve (a)) decreases and eventually disappears (in the alloys) on Ru atoms NN of Pd atoms. A reasonable estimation of RT-averaged values of s_0 for $0 < x \lesssim 0.15$ can be obtained by summing the contribution to $s_0(E_i)$ of hexagonal regions centered on each surface atom.[36] In contrast to the case of Pd-rich alloys, the use of this simple method is justified for Ru-rich alloys because only direct dissociation events are expected. The contribution of regions centered on Pd atoms can be safely neglected because of the low reactivity of Pd atoms, whereas the contribution of hexagons centered on Ru atoms surrounded only by Ru atoms can be taken equal to the sticking curve of H_2 on pure Ru(0001), $s_0^{x=0}(E_i)$.[17,37] The contribution of hexagons centered on Ru atoms NN of a Pd atom (Ru_{NN}) can be taken as $s_0^{x=0}(E_i + 8\ \text{meV})$ since, as shown in Fig. 5, the early activation barrier for H_2 dissociation on top of them is 8 meV lower than on top of Ru atoms in pure Ru(0001) (see the ESI† for further details). The RT-averaged s_0 values obtained in this way are shown in Fig. 1a. The computed initial slope, ds_0/dx, is relatively small (positive) and consistent with the experimental one.[7] It is important to note that the difference between the s_0 values obtained for $x = 0$ and $x = 0.14$ is similar to the typical error bars of the measured data. We thus conclude that for Ru-rich alloys the passivation due to isolated Pd atoms is slightly overcompensated by the increased reactivity of their NN Ru atoms.

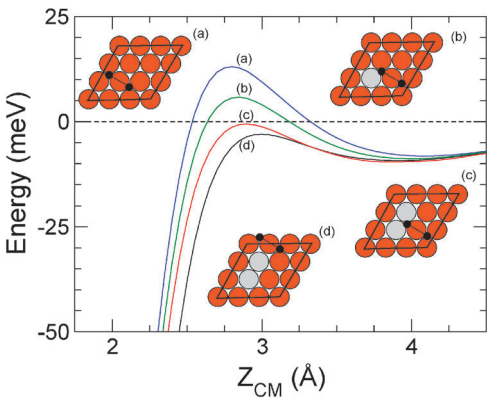

Fig. 5 Minimum energy DPs for molecular hydrogen interacting with: (a) pure Ru(0001), (b) $Pd_{0.11}Ru_{0.89}/Ru(0001)$, and (c) and (d) $Pd_{0.22}Ru_{0.78}/Ru(0001)$. The molecular configurations (parallel to the surface) are illustrated in the insets, where orange (grey) circles represent Ru (Pd) atoms.

The previous analysis of the reactivity of Ru- and Pd-rich surface alloys provides a sound explanation for the intriguing behavior of s_0 observed in the *limit* cases $x < 0.15$ and $x > 0.85$ respectively. For intermediate Pd (or Ru) concentrations (*e.g.* $x \sim 0.5$), Pd and Ru aggregates of different sizes coexist in $Pd_xRu_{1-x}/Ru(0001)$.[7] On the one hand, large Ru aggregates, in which most atoms are as reactive as in pure Ru(0001), must contribute to a global surface reactivity close to that of Ru(0001). On the other hand, large Pd aggregates made of barely reactive Pd atoms (like in the full Pd monolayer) are inert but favor dissociative adsorption on the activated Ru atoms placed in the boundary between Pd and Ru aggregates. Though a precise evaluation of s_0 in this case is extremely involved, it is likely that the latter opposite effects cancel each other leading to a s_0 value close to that of $H_2/Ru(0001)$ as observed in the experiments.

To summarize, we have shown that the environment dependent reactivity of Ru atoms in $Pd_xRu_{1-x}/Ru(0001)$ is responsible for the peculiar step-like dependence of the reactive sticking probability of molecular hydrogen as a function of the Pd concentration. In contrast with pure Pd surfaces, Pd atoms are highly unreactive due to both strain and ligand electronic effects. However, Ru atoms surrounded by Pd atoms become more reactive than in pure Ru(0001). For Pd-rich surface alloys, the high reactivity of isolated Ru atoms together with dynamic trapping of low energy molecules first encountering non-reactive Pd patches gives rise to a global reactivity that sharply decreases in a small range of Pd concentration, $0.9 \gtrsim x \leq 1$. In the case of surface alloys with higher Ru contents, the existence of larger Ru aggregates makes them more similar to pure Ru(0001). In addition, the passivating effect of Pd atoms is compensated by the fact that they turn their nearest neighbor Ru atoms more active (in terms of activation barriers for H_2 dissociation) than in the case of pure Ru(0001). Then, in stark contrast with the H chemisorption energy, the global surface alloy reactivity for H_2 dissociation barely depends on the Pd concentration. Thus, environment-dependent effects on the reactivity of H_2 on single atoms allow one to get around the constraints that are behind the widely used Brønsted–Evans–Polanyi relationship, which entails the simultaneous decrease of activation barriers (in favor of a given elementary catalytic step) and the increase of the products' bond strengths (to detriment of the forthcoming elementary catalytic steps). This highlights the huge potentiality of bimetallic surface alloys for the design of more efficient catalysts.

Acknowledgements

The authors acknowledge M. Wijzenbroek and Prof. G.-J. Kroes (Leiden University, The Netherlands) for providing us with the unpublished QCT results for $H_2/Ru(0001)$ shown in Fig. 8 in the ESI,† Prof. R. J. Behm for his useful comments about this work, and the *CCT-Rosario* Computational Center, member of the

High Performance Computing National System (SNCAD, MincyT-Argentina) and the CCC-UAM for allocation of computer time. This work has been supported by ANPCyT (project PICT Bicentenario No. 1962), CONICET (project PIP 0667), UNR (project PID ING235), MICINN (projects FIS2010-15127, FIS 2010-18847, CTQ2010-17006 and CSD2007-00010), CAM (project S2009/MAT1726), MEC and AECID (project A2/039631/11).

References

1 M. Mavrikakis, B. Hammer and J. Nørskov, *Phys. Rev. Lett.*, 1998, **81**, 2819.
2 B. E. Hayden and A. Hodgson, *J. Phys.: Condens. Matter*, 1999, **11**, 8397.
3 J. Greeley and M. Mavrikakis, *Nat. Mater.*, 2004, **3**, 810.
4 M. Lischka, C. Mosch and A. Groß, *Electrochim. Acta*, 2007, **52**, 2219.
5 G. Laurent, H. F. Busnengo, P. Rivière and F. Martín, *Phys. Rev. B: Condens. Matter Mater. Phys.*, 2008, **77**, 193408.
6 J. Chen, C. Menning and M. Zellner, *Surf. Sci. Rep.*, 2008, **63**, 201.
7 H. Hartmann, T. Diemant, A. Bergbreiter, J. Bansmann, H. Hoster and R. J. Behm, *Surf. Sci.*, 2009, **603**, 1439.
8 H. L. Tierney, A. E. Baber, J. R. Kitchin and E. C. H. Sykes, *Phys. Rev. Lett.*, 2009, **103**, 246102.
9 G. Laurent, C. Díaz, H. F. Busnengo and F. Martín, *Phys. Rev. B: Condens. Matter Mater. Phys.*, 2010, **81**, 161404.
10 G. Kyriakou, M. B. Boucher, A. D. Jewell, E. a. Lewis, T. J. Lawton, A. E. Baber, H. L. Tierney, M. Flytzani-Stephanopoulos and E. C. H. Sykes, *Science*, 2012, **335**, 1209.
11 C. Díaz, F. Martín, G. J. Kroes, M. Minniti, D. Farías and R. Miranda, *J. Phys. Chem. C*, 2012, **116**, 13671.
12 M. Minniti, D. Farías, P. Perna and R. Miranda, *J. Chem. Phys.*, 2012, **137**, 074706.
13 J. Libuda and H. Freund, *Surf. Sci. Rep.*, 2005, **57**, 157.
14 D. Farías and K. H. Rieder, *Rep. Prog. Phys.*, 1998, **61**, 1575.
15 These T_{des} values correspond to the maximum desorbing flux of D_2 recorded in temperature programmed desorption experiments for a low initial D coverage as obtained after a D_2 exposure of 0.3×10^{-6} mbar s.[7] The reported atomic hydrogen binding energies are taken with respect to 1/2 H_2 far from the surface and with positive values corresponding to exothermic dissociative adsorption.
16 B. Poelsema and G. Comsa, Scattering of Thermal Energy Atoms from Disordered Surfaces, *Springer Tracts in Modern Physics*, Springer-Verlag, Berlin, 1989, vol. 115.
17 J. K. Vincent, R. A. Olsen, G. J. Kroes, M. Luppi and E. J. Baerends, *J. Chem. Phys.*, 2005, **122**, 044701.
18 M. Luppi, R. A. Olsen and E. J. Baerends, *Phys. Chem. Chem. Phys.*, 2006, **8**, 688.
19 I. M. N. Groot, H. Ueta, M. J. T. C. van der Niet, a. W. Kleyn and L. B. F. Juurlink, *J. Chem. Phys.*, 2007, **127**, 244701.
20 A. Michaelides, Z.-P. Liu, C. J. Zhang, A. Alavi, D. a. King and P. Hu, *J. Am. Chem. Soc.*, 2003, **125**, 3704.
21 T. Bligaard, J. Nørskov, S. Dahl, J. Matthiesen, C. Christensen and J. Sehested, *J. Catal.*, 2004, **224**, 206.
22 G. Kresse and J. Furthmüller, *Comput. Mater. Sci.*, 1996, **6**, 15.
23 G. Kresse and J. Furthmüller, *Phys. Rev. B: Condens. Matter Mater. Phys.*, 1996, **54**, 11169.
24 G. Kresse and D. Joubert, *Phys. Rev. B: Condens. Matter Mater. Phys.*, 1999, **59**, 1758.
25 P. E. Blöchl, *Phys. Rev. B: Condens. Matter Mater. Phys.*, 1994, **50**, 17953.
26 J. P. Perdew, K. Burke and M. Ernzerhof, *Phys. Rev. Lett.*, 1997, **78**, 1396.
27 M. Methfessel and A. T. Paxton, *Phys. Rev. B: Condens. Matter Mater. Phys.*, 1989, **40**, 3616.
28 N. W. Ashcroft and N. D. Mermin, *Solid State Physics*, Holt, Rinehart and Winston, 1976.
29 J. P. Perdew, *Electronic Structure of Solids '91*, Akademie-Verlag, Berlin, 1991.
30 G. Laurent, F. Martín and H. F. Busnengo, *Phys. Chem. Chem. Phys.*, 2009, **11**, 7303.
31 H. F. Busnengo, C. Crespos, W. Dong, J. C. Rayez and A. Salin, *J. Chem. Phys.*, 2002, **116**, 9005.
32 The results obtained for $H_2(\nu = 0, J = 1,2,3)$ and $D_2(\nu = 0, J = 0,1,2,3)$ are similar and can be found in the ESI†.
33 The threshold of 0.12 eV in the case of $H_2/Pd_{ML}/Ru(0001)$ (*i.e.* 0.1 eV lower than the lowest activation energy barrier) is simply due to vibrational softening[5].
34 M. A. Di Césare, H. F. Busnengo, W. Dong and A. Salin, *J. Chem. Phys.*, 2003, **118**, 11226.
35 For D_2 we have obtained very similar results that are included in the ESI†.
36 M. Ramos, M. Batista, A. Martnez and H. Busnengo, *Springer Series in Surface Science 50. Dynamics of Gas-Surface Interactions*, Springer, 2013.
37 M. Wijzenbroek and G.-J. Kroes, private communication.

